# Cooperative Adaptive Cruise Control With Unconnected Vehicle in the Loop

Zheng Chen<sup>®</sup>, Graduate Student Member, IEEE, and Byungkyu Brian Park<sup>®</sup>, Senior Member, IEEE

Abstract—To improve the usability of cooperative adaptive cruise control (CACC) in the mixed traffic, a CACC algorithm with unconnected vehicle in the loop (CACCu) is proposed. Unlike the traditional CACC that requires a connected preceding vehicle or otherwise degrades to adaptive cruise control (ACC), CACCu aims to closely follow an unconnected preceding vehicle utilizing the information from the further (connected) preceding vehicle. Moreover, CACCu can robustly maintain string stability given various behaviors of unconnected preceding vehicles, without requiring identification process or extra information on the unconnected vehicles. For the sake of simplicity, this paper starts with CACCu in the three-vehicle sandwich scenario (i.e., one unconnected vehicle is in between of two connected vehicles), but derivatively, this control design is extended and evaluated in multiple-unconnected-vehicle cases. It is proven that by attaching a filter of "virtual preceding vehicle" to the original feedforward filter, the CACCu vehicle can stay string-stable at a gap significantly shorter than that required by ACC, given almost all kinds of car-following behaviors of the unconnected vehicle. At last, the favorable properties of CACCu are validated in high-fidelity simulations using real vehicle trajectory data and a physics-based vehicle dynamics model. The results show that CACCu outperforms existing ACC and acceleration-based connected cruise control (CCC) in string stability, ride comfort, safety maintenance, and fuel consumption.

Index Terms—CACC, mixed traffic, unconnected vehicle, string stability.

#### I. Introduction

UTOMATED vehicle (AV) has been developed for several decades. Some partially-automated driving applications such as adaptive cruise control (ACC) have been commercialized and massively equipped in new vehicles [1]. Using onboard sensors (e.g., radar or lidar), ACC can automatically control the vehicle's longitudinal motion to maintain a safe gap from the preceding vehicle, thus the labor intensity of drivers can be greatly reduced.

AV can be upgraded to Connected and Automated Vehicle (CAV) when vehicle-to-vehicle (V2V) and/or vehicle-to-infrastructure (V2I) communication devices are installed. These communications enable CAV to run in a cooperative way with other vehicles. One of the critical CAV applications

Manuscript received November 26, 2019; revised May 6, 2020, August 15, 2020, and November 19, 2020; accepted November 23, 2020. Date of publication December 17, 2020; date of current version May 3, 2022. This work was supported in part by the GRL Program through the NRF of Korea under Grant 2013K1A1A2A02078326 and by the National Science Foundation under Grant CMMI-2009342. The Associate Editor for this article was D. Wu. (Corresponding author: Zheng Chen.)

The authors are with the Link Lab, University of Virginia, Charlottesville, VA 22904 USA, and also with the Department of Engineering Systems and Environment, University of Virginia, Charlottesville, VA 22904 USA (e-mail: zc4ac@virginia.edu; bp6v@virginia.edu).

Digital Object Identifier 10.1109/TITS.2020.3041840

is Cooperative Adaptive Cruise Control (CACC) which is developed on top of existing ACC system. CACC utilizes the feedforward signal from preceding vehicle(s) to quickly respond to the speed perturbation from downstream. This feature allows the CACC vehicle to stably travel in short time gaps (e.g., 0.6s [2]) that could not be achieved easily by ACC or human drivers. In the past decades, a variety of CACC systems with different architectures and control methods have been proposed [3]. Based on communication topology, CACC can be briefly divided into three categories: predecessor-following (PF) CACC [4] which only communicates with the nearest preceding vehicle, predecessor-leaderfollowing (PLF) CACC [2] which communicates with both the nearest preceding vehicle and platoon leader, and multiplepredecessor-following (MPF) CACC [5], [6] which requires communications with multiple or all the preceding vehicles. As for the control method, rule-based linear control (e.g., Proportional-Derivative (PD) controller [2], [4]) has been frequently adopted in CACC demonstration, while multiobjective optimization-based control (e.g., Model Predictive Control (MPC) [7], [8]) is emerging with the enhancement of onboard computing capability. A variety of CACC systems were tested in Grand Cooperative Driving Challenge (GCDC) 2011 [9] and 2016 [10], which positively demonstrated that heterogeneous CACC vehicles can be compatible and implemented together in the traffic. To prepare CACC for the final large-scale deployment, research attentions have also been paid to the issues of communication unreliability [11]-[14], cyber-attacks [15], [16], and formation/organization of CACC platoon [17]–[20].

The potential benefits of CACC have been extensively shown in previous studies. The most appealing impact of CACC is doubling the throughput on both highways [21] and urban roads [22]. Other significant benefits include reducing 6%~11% fuel consumption [23] and improving traffic flow quality [24]. However, many research efforts also pointed out that benefits of CACC may not be easily unleashed in the near future when CAVs are travelling together with large numbers of non-CAVs in the traffic [21], [22], [25]–[28]. A technical limitation shared by most of CACC systems is that the nearest preceding vehicle must be a CAV or at least a connected vehicle (CV) [17]. This operating requirement seriously limits the usability of vehicular connectivity because CACC has to fall back to ACC when encountering an unconnected preceding vehicle.

To partially maintain the favorable properties of CACC when the communication from preceding vehicle becomes unavailable or unstable, [29] proposed graceful degradation of CACC (dCACC) based on estimated preceding vehicle's

acceleration using onboard radar. With dCACC, the equipped vehicle can stably maintain a short gap which is less than a half of that needed for ACC. Nevertheless, the quality of radar measurement was shown as a main drawback of dCACC. Because radar is not designed to measure the acceleration, the feedforward signal from radar, instead of from the communication, often contains a lot of noise. This noise impaired the smoothness of the vehicle trajectory. As such, the ride comfort was sacrificed.

Connected cruise control (CCC) [30] was proposed to explore the benefits of communication with out-of-sight preceding vehicles when the nearest preceding vehicle is unconnected. However, the CCC requires the behavior pattern of unconnected vehicle to be adequately known or identified [31] before the CCC can work properly. The identification process could take tens of seconds [31], and even after that, the car-following behavior of the unconnected vehicle is unlikely to remain time-invariant if it is driven by human. The same limitation was seen in a centralized CACC [32].

An optimal CCC [33] was proposed to represent the time-variant behaviors of the preceding vehicle with mean values and distributions of human parameters, but it costed even longer time to identify such distributions. Actually, this can be problematic for control design because the human parameters were not perfectly stochastic, i.e., they can continuously deviate from their past mean values for tens of seconds [33], which is long enough to cause unexpected consequences (such as loss of string stability). On the other hand, while the design of existing CACC systems is based on zero-spacing-error rule and the strong string stability of individual vehicle [9], the emphasis of CCC often lays on head-to-tail string stability of platoon, which could greatly suppresses the traffic turbulence but not necessarily help maintain the desired spacing for the individual vehicle [34].

In summary, the problem of CAV platooning in mixed traffic has attracted increasing research efforts but has not been properly addressed. The extra process of human behavior identification is one of the main restrictions on the existing approaches when faced with the large uncertainty in unconnected vehicles' car-following behaviors.

This paper proposes a new CACC algorithm, dubbed as CACC with Unconnected vehicle in the loop (CACCu). By utilizing the information from the further (connected) preceding vehicle, CACCu enables CAVs to closely and stably follow an unconnected preceding vehicle, thus the aforementioned benefits of CACC can be partially achieved. Moreover, CACCu is designed to robustly handle various unconnected vehicle's car-following behaviors, without requiring identification process or extra information on the unconnected vehicles. While CACCu will be extended and evaluated in more general scenarios later, this paper starts with the detailed control design and analysis of CACCu in three-vehicle sandwich scenario (i.e., an unconnected vehicle is in between of two connected vehicles), which is simple but with the highest probability to occur among the mixed platooning scenarios.

The rest of the paper is organized as follows: the second section describes the control design of the proposed CACCu;

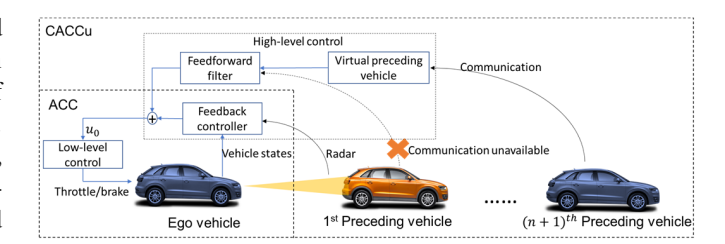


Fig. 1. General framework of CACCu.

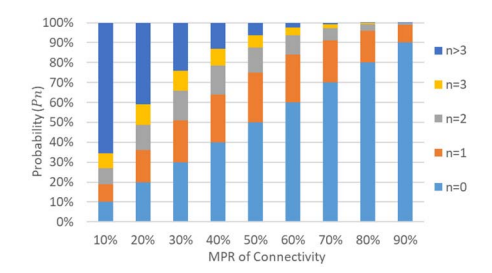


Fig. 2. Market Penetration Rata (MPR) of connectivity and the probability that the closest connected preceding vehicle is *n* vehicle(s) away.

the string stability of CACCu under the effects of different control gains, communication delay, and vehicle dynamics is discussed in the third section; the performance evaluation of CACCu is presented in the fourth section, which demonstrates the advantages of CACCu over existing ACC and acceleration-based CCC. The fifth section summarizes the main contributions and key findings of the research.

#### II. CONTROL DESIGN

### A. Framework

Typical CACC systems obtain the acceleration or desired acceleration of nearest preceding vehicle as a feedforward signal [35]. This feedforward signal can efficiently help eliminate spacing error (i.e., the difference between actual spacing and desired spacing), and thus enables safe driving at short gaps [9]. However, as shown in Fig. 1, when the ego vehicle encounters an unconnected preceding vehicle or vehicles, such feedforward signal is not available. Instead of degrading to ACC, the proposed CACCu turns to utilize the closest connected vehicle ahead (i.e., the  $(n+1)^{th}$  preceding vehicle in Fig. 1) as the source of feedforward signal. An additional filter of "virtual preceding vehicle(s)" is inserted before the original feedforward filter of CACC, to compensate for the effects of n unconnected preceding vehicle(s) in between. Assuming random clustering of vehicles [36], the probability  $(P_n)$  of having different n (i.e., the number of unconnected preceding vehicles) for a CAV is directly linked to Market Penetration Rate (MPR) of vehicular connectivity. Fig. 2 shows how  $P_n$  varies with n and MPR, where  $P_n$  is calculated as  $MPR \cdot (1 - MPR)^{n-1}$ . It can be seen that enabling CACCu for n = 1 (i.e., three-vehicle sandwich scenario) could make the most considerable complement to CACC (n = 0). Hence, a special emphasis is laid on such three-vehicle sandwich scenario.

In addition, a bi-level control structure is needed due to the nonlinearity of vehicle dynamics. The high-level control decides the desired acceleration  $(u_0)$ , while the low-level control determines how to actuate the throttle and brake to achieve this desired acceleration. For high-level control, a linear time-invariant control law is pursued in this study for easy parameterization and implementation. As shown in Fig. 1, the proposed CACCu can be directly extended from an existing CACC system with minimum re-design (i.e., only inserting a "virtual preceding vehicle"). Such design of CACCu would also facilitate the straightforward performance comparisons with ACC using exactly the same feedback configuration.

In the rest of this section, the three key components of CACCu are described respectively, including the consideration in human car-following behaviors and the designs of high/low-level controls.

# B. Stochastic Car-Following Behaviors of Unconnected Vehicle

It is intuitive that a driver takes action based on the intervehicle spacing and relative speed to the preceding vehicle, with perception/reaction delay. In this sense, the linearized optimal velocity model (OVM) [37], which considers control gains regarding spacing and speed, human delay, and the desired time headway, is the most basic linear model of carfollowing behavior. In fact, other frequently used car-following models (e.g., intelligent driver model) can also be linearized into the same form of OVM [37]. Therefore, the OVM is adopted in this study to describe car-following behaviors of the unconnected human-driven vehicle around a traffic equilibrium (i.e., steady state with constant velocity):

$$h_{1}(t) = x_{2}(t) - x_{1}(t) - l_{2}$$

$$\ddot{x}_{1}(t) = \alpha_{1} \left( \frac{1}{t_{1,h}} h_{1}(t - \varphi_{1}) - \dot{x}_{1}(t - \varphi_{1}) \right)$$

$$+ \beta_{1} \dot{h}_{1}(t - \varphi_{1}) + e_{m}(t)$$
(1)

where t is time,  $\dot{*}$  denotes the variable's derivative in respect to time,  $x_1(t)$  and  $x_2(t)$  are locations of the human-driven vehicle and its preceding vehicle,  $h_1$  is the inter-vehicle spacing, with  $l_2$  being the length of preceding vehicle,  $\alpha_1$  and  $\beta_1$  are human control gains,  $\varphi_1$  is the human reaction time,  $\frac{1}{t_{1,h}}$  is spacing policy slope with  $t_{1,h}$  being the desired time gap of the human driver, and  $e_m(t)$  is a noise term representing the unmodeled actions of the human driver. Model (1) indicates that the human driver desires a velocity-dependent spacing, and regulates the spacing error and speed difference from the preceding vehicle simultaneously.

It should be noted that the human parameters in (1) vary from person to person, and even for one single driver, they may change stochastically over time. To incorporate the variation of human parameters yet avoid the time-consuming identification [31], [33], a realistic and convenient assumption is adopted in this study.

Assumption 1: the driver's car-following behavior should be represented by different  $\varphi_1$ ,  $\alpha_1$ ,  $\beta_1$  and  $t_{1,h}$  in every short period of regulation (i.e., the time from the traffic equilibrium being disturbed until a new equilibrium is reached).

In other words, the human driver responds to each speed perturbation in different ways, but the driver's behavior during one regulation period is relatively stable. This assumption requires that any control design involving human driver should be able to handle a range of human parameters instead of a specific combination. Meanwhile, the stochastic behavior of human driver is approximated by a sequence of linear timeinvariant systems (thus transfer functions exist), which will bring great convenience in the control design and analysis.

Taking the Laplace transform of (1) with zero initial conditions, the transfer function of the human-driven vehicle in each regulation period can be obtained:

$$T_1(s) = \frac{L(x_1(t))}{L(x_2(t))} = \frac{K_1(s)}{s^2 e^{\varphi_1 s} + K_1(s) + \alpha_1 s}$$
(2)

where  $L(\cdot)$  denotes Laplace transform and

$$K_1(s) = \frac{\alpha_1}{t_{1,h}} + \beta_1 s$$

To incorporate all kinds of human drivers, the possible ranges of human parameters reported in existing studies are summarized below:

- The preferred time gap t<sub>1,h</sub> of highway drivers is found to be 1~2s [38].
- The human delay φ<sub>1</sub> was reported to be 0.5~1.5s in [39], while [40] found the brake delay in normal case to be 0.92~1.93s, and acceleration delay to be 0.4~1.5s.
- For the human control gains  $\alpha_1$  and  $\beta_1$ , previous literature [30], [41] used the average value of 0.6 and 0.9, which are derived from macroscopic data. However, field test [33] determined the average values of  $\alpha_1$  and  $\beta_1$  to be 0.2 and 0.4. Considering the large difference between these two sets of value, the average values of 0.4 and 0.65 can be assumed for  $\alpha_1$  and  $\beta_1$ , respectively, as compromise.

It is worth noting that different human parameters are not likely to appear with the equal probability. In control design, the recurrent combinations of human parameters should be given more considerations. Thus, a probability model is needed to capture the uneven distribution of human parameters. Although with limited number of participating drivers, [33] has identified bell-shaped distributions of human parameters and treated them as independent. In this paper, the human parameters are assumed to follow independent normal distributions, whose means and variances are determined based on the aforementioned ranges of human parameters.

Assumption 2: for the population of all drivers, the  $\varphi_1$ ,  $\alpha_1$ ,  $\beta_1$  and  $t_{1,h}$  follow independent normal distribution as below:

- Desired time gap  $t_{1,h} \sim N(1.5, 0.25^2)$ , which means it has 95% probability to be 1 $\sim$ 2;
- Human delay  $\varphi_1 \sim N(1, 0.25^2)$ , which means it has 95% probability to be 0.5 $\sim$ 1.5;
- Human gain  $\alpha_1 \sim N(0.4, (\frac{0.4}{2.6})^2)$ , which means it has 98% probability to be 0~0.8 and only 1% probability to be negative;
- Human gain  $\beta_1 \sim N(0.65, (\frac{0.65}{2.6})^2)$ , which means it has 98% probability to be  $0 \sim 1.3$  and only 1% probability to be negative.

Nevertheless, the design of CACCu does not rely on a specific type of probability model, as shown in the rest of paper. *Assumption* 2 is free to be modified or replaced when there are new findings on human parameters.

# C. High-Level Control of CACCu Vehicle

CACCu follows the basic structure of predecessor-following CACC which is featured by the feedforward-feedback control and velocity-dependent spacing policy [4]. The main difference is that the feedforward signal is from the further preceding vehicle instead of the 1<sup>st</sup> one. Thus, the CACC feedforward filter needs to be modified. When the 2<sup>nd</sup> preceding vehicle is a connected vehicle, the car-following behavior of CACCu vehicle is as below:

$$h_{0}(t) = x_{1}(t) - x_{0}(t) - l_{1}$$

$$h_{0,d}(t) = t_{0,h}\dot{x_{0}}(t) + h_{0,st}$$

$$e_{0}(t) = h_{0}(t) - h_{0,d}(t)$$

$$u_{0}(t) = k_{0,p}e_{0}(t) + k_{0,d}\dot{e_{0}}(t) + f_{0}(\ddot{x}_{2}(t - \theta_{0}))$$

$$\ddot{x}_{0}(t) = g_{0}(u_{0}(t))$$
(3)

where  $x_0(t)$  is the location of the ego vehicle,  $h_0$  is the spacing from the preceding vehicle, with  $l_1$  being the length of the 1<sup>st</sup> preceding vehicle,  $h_{0,d}(t)$  is the desired spacing,  $h_{0,st}$  is the standstill spacing,  $t_{0,d}$  is the desired time gap,  $e_0(t)$  is the spacing error,  $k_{0,p}$  and  $k_{0,d}$  are the gains of the proportional-derivative (PD) feedback controller,  $f_0(\cdot)$  is the new feedforward filter,  $\ddot{x}_2$  is the acceleration of the second preceding vehicle, and  $\theta_0$  is the communication delay,  $g_0(\cdot)$  is the vehicle dynamics of the CACCu vehicle.

Accompanied by a proper low-level controller [42], the longitudinal vehicle dynamics  $g_0(\cdot)$  can be approximated by a first-order delayed system:

$$g_0(u_0(t+\phi_0)) + \tau_0 \dot{g}_0(u_0(t+\phi_0)) = u_0(t)$$
 (4)

The corresponding transfer function in Laplace domain is:

$$G_0(s) = \frac{L(x_0(t))}{L(u_0(t))} = \frac{1}{s^2(1+\tau_0 s)}e^{-\phi_0 s}$$
 (5)

where  $\tau_0$  is the system lag and  $\phi_0$  is the actuator delay.

The  $f_0(\cdot)$  should be designed so that the spacing error can be eliminated. According to (3) with zero initial conditions, the Laplace transform of spacing error can be obtained:

$$L(e_0(t)) = \frac{1}{1 + G_0(s)K_0(s)H_0(s)}L(x_1(t)) - \frac{D_0(s)G_0(s)F_0(s)H_0(s)s^2}{1 + G_0(s)K_0(s)H_0(s)}L(x_2(t))$$
(6)

where

$$F_0(s) = L(f_0(t))$$

$$K_0(s) = k_{0,p} + k_{0,d}s$$

$$H_0(s) = 1 + t_{0,h}s$$

$$D_0(s) = e^{-\theta_0 s}$$

Let  $L(e_0(t)) = 0$ , then:

$$L(x_1(t)) - D_0(s) G_0(s) F_0(s) H_0(s) s^2 L(x_2(t)) = 0$$

And thus

$$F_0(s) = \frac{1}{D_0(s)G_0(s)H_0(s)s^2} \frac{L(x_1(t))}{L(x_2(t))}$$
$$= \frac{1}{D_0(s)G_0(s)H_0(s)s^2} T_1(s)$$

However, the exact value of communication delay  $\theta_0$  and human parameters are unpredictable in real world. Thus, by setting  $\theta_0 = 0$ , a feasible feedforward filter is:

$$F_0(s) = \frac{1}{G_0(s) H_0(s) s^2} T_1'(s)$$
 (7)

where  $\frac{1}{G_0(s)H_0(s)s^2}$  is the original feedforward filter used in CACC [4], and  $T_1'(s)$  is the additional filter of a "virtual preceding vehicle" that has the same form of  $T_1(s)$ :

$$T_1'(s) = T_1'(\alpha_1', \beta_1', \varphi_1', t_{1,h}', s)$$
(8)

where  $\alpha_1', \beta_1', \varphi_1', t_{1,h}'$  are the parameters of the "virtual preceding vehicle."

Since there is little chance to make  $T_1'(s)$  exactly equal to T(s) (thus to perfectly predict the acceleration of the first preceding vehicle), parameters  $(\alpha_1', \beta_1', \varphi_1', t_{1,h}')$  are left to be tuned so that CACCu vehicle can stay string-stable for a vast range of unconnected vehicle behaviors described by  $(\alpha_1, \beta_1, \varphi_1, t_{1,h})$ . Obviously, when the feedforward signal comes from more distant vehicle (i.e., when there are multiple unconnected vehicles in between),  $T_1(s)$  and  $T_1'(s)$  should be replaced by the combined transfer function of multiple human-driven vehicles, and tuning of this transfer function will require more effort, as shown later in the fourth Section.

Finally, the transfer function of the CACCu vehicle can be derived combining (3) and (7):

$$T_0(s) = \frac{L(x_0(t))}{L(x_1(t))}$$

$$= \frac{H_0(s)G_0(s) K_0(s) + D_0(s) T_1'(s)/T_1(s)}{H_0(s)(1 + H_0(s)G_0(s) K_0(s))}$$
(9)

As comparison, the existing CACC systems [4] let  $f_0(\ddot{x}_2(t-\theta_0)) = 0$  when following an unconnected vehicle. This setting degrades the CACC to ACC and leads to a transfer function of:

$$T_0(s) = \frac{L(x_0(t))}{L(x_1(t))} = \frac{G_0(s) K_0(s)}{1 + G_0(s) K_0(s) H_0(s)}$$
(10)

# D. Low-Level Control of CACCu Vehicle

According to (3), the high-level controller outputs the desired acceleration to the vehicle dynamics. However, the longitudinal motion of vehicle is directly controlled by the throttle and brake. Thus, a low-level controller is needed to convert the desired acceleration to proper throttle and brake action so that the command from high-level controller can be accurately achieved. A typical low-level controller [42] utilizes the inverse engine torque map and a set of feedforward signals (i.e., vehicle speed, engine speed, and transmission ratio) to pre-compensate the nonlinear behaviors of the engine, transmission system, air drag and rolling resistance, leading to a first-order linear relationship between desired acceleration and actual acceleration as described by (4), and a third-order linear relationship between desired acceleration and vehicle position as described by (5).

# III. STRING STABILITY ANALYSIS

String stability is one of the most important design goal of longitudinal vehicle control. In this study, CACCu is required to guarantee string stability not only for a single combination of  $\alpha_1$ ,  $\beta_1$ ,  $\varphi_1$ ,  $t_{1,h}$  but for broad ranges of them. A widely-accepted version of string stability is defined in [4], that is, given any disturbance in the longitudinal movement of preceding vehicle, the following vehicle should not amplify this disturbance. While string stability can also be defined in terms of spacing error or control input, they are less practical when human driver is involved. According to [4], the string stability of ego vehicle is fulfilled when the magnitude of its frequency response is always no greater than 1:

SS

$$= \|T_{0}(j\omega)\|_{\infty}$$

$$= \left\|\frac{H_{0}(j\omega)G_{0}(j\omega)K_{0}(j\omega) + D_{0}(j\omega)T'_{1}(j\omega)/T_{1}(j\omega)}{H_{0}(j\omega)(1 + H_{0}(j\omega)G_{0}(j\omega)K_{0}(j\omega))}\right\|_{\infty}$$

$$\leq 1 \tag{11}$$

where  $\|\cdot\|_{\infty}$  denotes the maximum magnitude over all frequency  $\omega$ , and j is the imaginary unit. Because  $T_0(j\omega) = \frac{L(x_0(t))}{L(x_1(t))} = \frac{L(\dot{x}_0(t))}{L(\dot{x}_1(t))} = \frac{L(\ddot{x}_0(t))}{L(\ddot{x}_1(t))}$ , condition (11) can be approximately interpreted as that given any perturbation from the downstream, the speed or acceleration disturbance of ego vehicle caused by the perturbation should not exceed that of the preceding vehicle.

To measure CACCu's robustness against the uncertain carfollowing behaviors of preceding vehicle, String Stability Ratio (SSR) is defined as the probability that ego vehicle stays string-stable given all different kinds of  $(\alpha_1, \beta_1, \varphi_1, t_{1,h})$ . By definition, SSR can be computed as an integral of the probability density over all the string-stable combinations of  $(\alpha_1, \beta_1, \varphi_1, t_{1,h})$ :

$$SSR = \int \int \int \int p(\alpha_1, \beta_1, \varphi_1, t_{1,h}) \xi(SS) d\alpha_1 d\beta_1 d\varphi_1 dt_{1,h}$$
(12)

where

$$\xi(SS) = \begin{cases} 1 & if \ SS \le 1 \\ 0 & if \ SS > 1 \end{cases}$$

 $p\left(\alpha_1, \beta_1, \varphi_1, t_{1,h}\right)$  is the joint probability density function (PDF) of human parameters, and SS is the string stability determinant defined by (11). According to Assumption 2,  $p\left(\alpha_1, \beta_1, \varphi_1, t_{1,h}\right)$  can be calculated as the product of PDFs of all the human parameters:

$$p\left(\alpha_{1}, \beta_{1}, \varphi_{1}, t_{1,h}\right) = \frac{1}{0.25 \cdot \sqrt{2\pi}} \exp\left(-\frac{\left(t_{1,h} - 1.5\right)^{2}}{2 \cdot 0.25^{2}}\right)$$

$$\cdot \frac{1}{0.25 \cdot \sqrt{2\pi}} \exp\left(-\frac{\left(\varphi_{1} - 1\right)^{2}}{2 \cdot 0.25^{2}}\right)$$

$$\cdot \frac{1}{\left(\frac{0.4}{2.6}\right) \cdot \sqrt{2\pi}} \exp\left(-\frac{\left(\alpha_{1} - 0.4\right)^{2}}{2 \cdot \left(\frac{0.4}{2.6}\right)^{2}}\right)$$

$$\cdot \frac{1}{\left(\frac{0.65}{2.6}\right) \cdot \sqrt{2\pi}} \exp\left(-\frac{\left(\beta_{1} - 0.65\right)^{2}}{2 \cdot \left(\frac{0.65}{2.6}\right)^{2}}\right) \quad (13)$$

To obtain an ideal SSR, the CACCu vehicle should not only use optimal virtual vehicle  $T'_1$  but also choose proper feedback controller  $K_0$  and spacing policy  $H_0$  based on the operating condition, i.e., the vehicle dynamics  $G_0$  and average communication delay  $D_0$ . Higher control gains in  $K_0$  typically

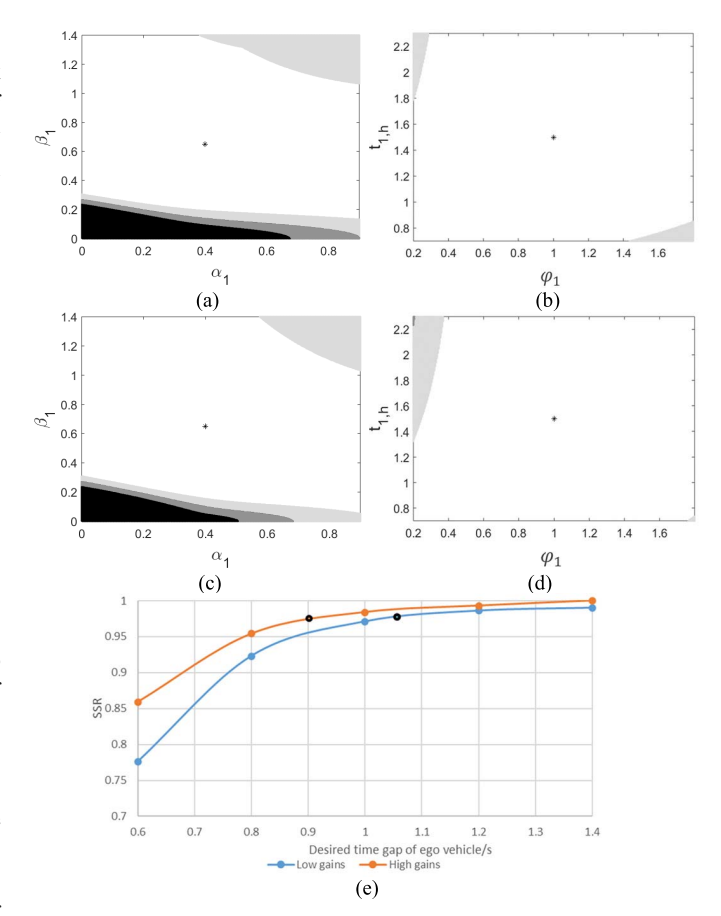


Fig. 3. The string-stable range of human parameters and SSR under different control gains and desired time gaps. (a) Low gains. (b) Low gains. (c) High gains. (d) High gains. (e) SSR.

improve string stability, but meanwhile they lead to more aggressive behaviors and higher sensitivity to sensor noise, thus may impair the ride comfort. Two pairs of  $(k_{0,p},k_{0,d})$  adopted in field tests are considered here:

- Low gains used in field test [4]:  $k_{0,p} = 0.25, k_{0,d} = 0.5$ ;
- High gains used in field test [43]:  $k_{0,p} = 0.3, k_{0,d} = 0.7$ ;

First, the effects of desired time gap and control gains on the string stability are explored, assuming perfect vehicle dynamics  $\tau_0 = 0$  and  $\phi_0 = 0$  and perfect communication  $\theta_0 = 0$ . Due to the complexity of (11), the string-stable space of  $(\alpha_1, \beta_1, \varphi_1, t_{1,h})$  are derived numerically and shown in Fig. 3. Using MATLAB optimization toolbox,  $(\alpha'_1, \beta'_1, \varphi'_1, t'_{1,h})$  have been optimized to (0.99, 0.62, 0, 0.72) for CACCu with low gains and (0.76, 0.51, 0, 0.57) for CACCu with high gains.

Fixing  $\tau_0 = \phi_0 = \theta_0 = 0$ , Fig. 3 (a)~(d) show the string-stable ranges of the human parameters  $(\alpha_1, \beta_1, \varphi_1, \text{ and } t_{1,h})$  under low/high control gains. Blank area denotes the string-stable range when desired time gap of ego vehicle is set 0.8s; lighter/darker shaded area denotes the increased string-stable range when desired time gap of ego vehicle increases to 1.0s/1.2s; the darkest shaded area denotes the string-unstable range when desired time gap of ego vehicle is 1.2s. Fig. 3 (a), (c) show string-stable ranges of  $\alpha_1$  and  $\beta_1$  (when  $\varphi_1 = 1$ ,  $t_{1,h} = 1.5$ ) for low and high gains, respectively. Fig. 3 (b), (d) show string-stable ranges of  $\varphi_1$  and  $t_{1,h}$  (when  $\alpha_1 = 0.4$ ,  $\beta_1 = 0.65$ ) for low and

high gains, respectively. Fig. 3 (e) shows SSR for low/ high control gains when the desired time gap of ego vehicle is set  $0.6s\sim1.4s$ .

It can be seen from Fig.  $3(a)\sim(d)$  that CACCu can provide broad string-stable ranges of human parameters. Given certain  $t_{1,h}$  and  $\varphi_1$ , CACCu tends to lose its string stability when  $\beta_1$  and  $\alpha_1$  are both low or both high. Given certain  $\alpha_1$  and  $\beta_1$ , CACCu tends to lose its string stability when  $t_{1,h}$  is much larger than  $\varphi_1$  (i.e., the preceding vehicle has fast response but maintains a long gap) or the inverse case. On the other hand, the string-unstable area shrinks when longer desired gap and higher control gains are used. This is expected as the longer desired gap and higher control gains have been proven helpful for the string stability of ACC/CACC [4], [5], [44]. Fig. 3(e) further shows that the SSR climbs to 99.7% when the high gains (e.g., 0.3, 0.7) and a desired time gap of 1.2s are used, which means CACCu vehicle can keep string-stable given almost all kinds of unconnected preceding vehicle. As comparison, by using (10) it can be found that an ACC vehicle with the same control gains needs a time gap  $\geq$ 2.6s to maintain its string stability. This gap is more than twice the gap required by CACCu. From another perspective, when driving at the same desired gap, a CACCu vehicle can better attenuate the speed oscillation from downstream than an ACC vehicle can do.

Considering that string stability is not a safety-critical requirement, it will be too trivial to prepare the CACCu for any combination of  $\alpha_1$ ,  $\beta_1$ ,  $\varphi_1$ , and  $t_{1,h}$ , especially after knowing that the string-unstable areas are at the edge of the parameter space that has low probability to occur. For this reason, a "critical gap" is defined as the desired time gap which can guarantee string stability at 97.5% probability (i.e., SSR  $\geq$  97.5%). Driving at the critical gap, CACCu can offer a dominant capability to accommodate human uncertainty over previous research efforts. It cancels the necessity of human parameters identification in advance, while string stability can be fulfilled in most cases. It can be seen in Fig. 3(e) that the critical gaps for CACCu with low/high control gains are 0.9s/1.05s, respectively, when assuming perfect vehicle dynamics and communication. More conservative critical gap can also be defined and found in Fig. 3(e).

Then, the effects of communication delay and imperfect vehicle dynamics on string stability are investigated. The possible values of communication delay  $\theta_0$  and vehicle lag  $\tau_0$ , and actuator delay  $\phi_0$  according to previous field tests have been summarized in [35]:

$$0.02 \le \theta_0 \le 0.2, 0.1 \le \tau_0 \le 0.8, 0.02 \le \phi_0 \le 0.25$$

Fig. 4 shows the different critical gaps under communication delay of  $0{\sim}0.2s$  when fixing  $\tau_0=\phi_0=0$ . It can be found the communication delay has mild impact on the string stability. The critical gaps of CACCu with low and high both increase by 0.15s when the largest communication delay of 0.2s is present. If the V2V communication is conducted every 100ms and the zero-order hold (ZOH) is applied to the received message, an average communication delay of 50ms can be expected. In this case, the critical gap only increases by 0.05s in high-gain case.

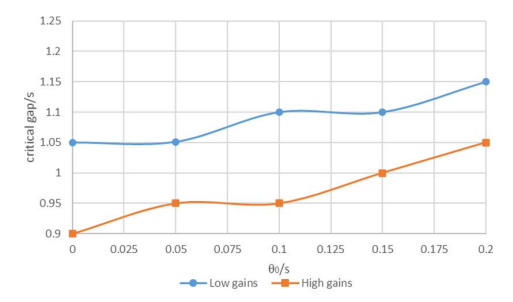


Fig. 4. Critical gaps under communication delay  $\theta_0 = 0 \sim 0.2$ s ( $\tau_0 = \phi_0 = 0$ ).

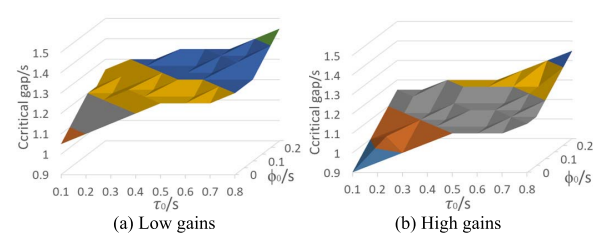


Fig. 5. The critical gaps under different vehicle dynamics for CACCu with low/ high control gains.

Fixing  $\theta_0 = 50$ ms, Fig. 5 shows the critical gaps under the effects of different vehicle lag  $\tau_0$  and actuator delay  $\phi_0$ . With low gains, the critical gap varies between 1.05s and 1.45s, while high gains shorten it to 0.9s  $\sim$ 1.35s.

In summary, the CACCu controller can be tuned by maximizing the string stable ratio (SSR). The analysis shows that the proposed CACCu is able to stay string-stable at a desired time gap significantly shorter than that required by ACC, when facing almost all kinds of unconnected preceding vehicles. This desirable property of CACCu holds true under the effects of imperfect communication and vehicle dynamics.

# IV. EVALUATION

Based on the proposed control structure in Section II and tuning method in Section III, CACCu are designed and evaluated in three scenarios, where the preceding connected vehicle is one, two, or three vehicles away from the ego vehicle. The human-driven vehicle trajectory data from Next Generation Simulation (NGSIM) [45] are adopted to construct the car-following scenarios for the evaluation. The NGSIM was launched by FHWA's Traffic Analysis Tools Program. It used high-resolution cameras to record trajectories of the vehicles on the real roads. The US Highway 101 (US 101) dataset was one dataset that reflected highway traffic condition. It contains the trajectories of vehicles in all 6 lanes within the 640-meter long study area during 45 minutes, which witnessed the buildup of congestion, the transition between uncongested and congested conditions, and full congestion during the rush hour. Trajectories of adjacent vehicles which entered the study area at 0 min, 10 min, 20 min, 30 min, and 35 min were extracted to simulate the car-following scenarios under various congestion levels. The ego vehicle is then assumed to follow these vehicles.

The control system of ego vehicle is developed in MATLAB-Simulink. As noted, the control system is divided into high-level and low-level systems. Besides CACCu, there are two more high-level systems to be evaluated, while the

low-level system remains the same. First as aforementioned, the ACC controller can be obtained by removing the feedforward term in CACCu, i.e., making  $f_0(\ddot{x}_2(t-\theta_0))=0$  in (3). Then, an acceleration-based CCC [30] can be developed by replacing the feedforward filter with a constant feedback gain:

$$f_0(\ddot{x}_2(t - \theta_0)) = \gamma \, \ddot{x}_2(t - \theta_0 - \sigma_2) \tag{14}$$

where  $\gamma$  is the feedback gain for the acceleration signal from second preceding vehicle, and  $\sigma_0$  is an intended delay for the acceleration feedback. The values of  $\gamma=0.5$  and  $\sigma_0=0.6$  are recommended in the original design [30]. However, as the original CCC assumed different feedback configuration,  $\gamma_2$  and  $\sigma_0$  need to be re-tuned in this study to ensure a fair comparison. Using our definition of SSR,  $\gamma$  and  $\sigma_0$  are adjusted to 0.42 and 0.65 respectively, for the highest probability to achieve head-to-tail string stability.  $\gamma$  and  $\sigma_0$  can be further adjusted for the scenarios where the other connected vehicle is two or three vehicles away.

Finally, to simulate the behavior of ego vehicle more realistically, the vehicle dynamics are represented by the physics-based Audi A8 model provided by PreScan [46], rather than the simplified models in (4) and (5). It should be noted that the simplified model is still needed for the design of high-level control.

According to the trajectories of ego vehicle and its first preceding vehicle, the ego vehicle's performance can be determined. The following measures of effectiveness (MOEs) are adopted in this study:

- String stability is measured by the count of speed overshoots (i.e., higher peak or lower valley values than the preceding vehicle's) during the ride;
- Safety/control accuracy is measured by spacing error of ego vehicle [43], [32]. Smaller amplitude of spacing error indicates the better capability of maintaining the desired gap and avoiding potential collision with preceding vehicle;
- Ride comfort is measured by the amplitude of ego vehicle's acceleration, considering that the comfort and acceleration were commonly linked in previous research [7], [2];
- The fuel consumed by the ego vehicle is estimated using Virginia-Tech fuel consumption model [47].

# A. NGSIM Data Pre-Processing

NGSIM trajectory data including position, speed, and acceleration profile of vehicles, among which the positions of vehicles were directly collected every 0.1s, while the speed and acceleration profiles of vehicles were derived from the position profiles. In the derivation of the speed and acceleration, the measurement error in position could be greatly propagated, leading to considerable noise in speed and acceleration profiles. It has been revealed that inconsistent speeds and unrealistic jerks (i.e., derivative of acceleration) can be frequently observed in the original NGSIM data, thus speed smoothing and recalculation of the acceleration is recommended before using the data [48].

In this study, the locally weighted scatterplot smoothing (LOWESS) is applied to the speed profiles of vehicles.

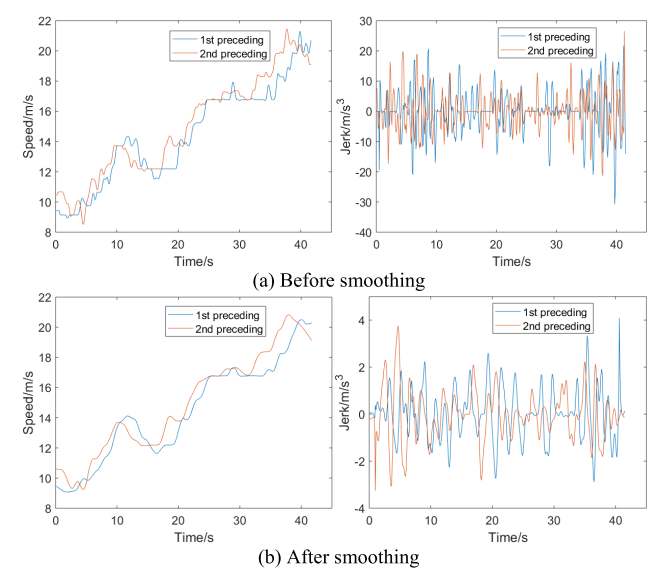


Fig. 6. Vehicle speed and jerk profiles before/after speed smoothing.

The size of sliding window is chosen as 2s. Fig. 6 shows the speed and jerk profiles of a pair of preceding vehicles before/after speed smoothing as an example. It can be seen that there are many sudden jumps of the speed in the original profiles. In addition, the jerk exceeded 15m/s<sup>3</sup> for many times, which is mechanically unrealistic [48]. After smoothing, the speed profiles of vehicles are less noisy, and the jerks are always below 15m/s<sup>3</sup>.

# B. Vehicle Dynamics Model

An Audi A8 sedan model from PreScan [46] plays as the ego vehicle in the evaluation. This physics-based vehicle model consists of engine, automatic gear box, 2-D chassis and other typical vehicle components. After the design of low-level control, the simplified vehicle dynamics model can be identified from the vehicle's response given a step acceleration command. MATLAB system identification toolbox is adopted to accomplish this identification. The identification result is:

$$G_0(s) = \frac{1}{s^2(1+0.12s)}e^{-0.2s}$$
 (15)

# C. Simulation Settings and Results

1) One Unconnected Vehicle: In the evaluation, the high control gains [0.3, 0.7] were adopted in all of CACCu, CCC and ACC. According to the identified vehicle dynamics (15) and Fig. 5 (b), a desired time gap of 1.1s should be sufficient for CACCu but apparently not for ACC and probably not for CCC (it is uncertain because human parameters of 1st preceding vehicle are unknown). However, to compare the performances of CACCu, CCC and ACC in the same situations, the desired time gaps for all three cases are set 1.1s. The sensor errors are modelled by normal distributions. The radar is assumed to be with 0.1m standard error on distance measurement and 0.1m/s on relative speed measurement [49]. The accelerometer on the 2<sup>nd</sup> preceding vehicle is assumed to have a standard error of 0.005m/s<sup>2</sup>. The communication delay is assumed to be 0.05s.

The results of the 5 simulation runs are summarized in Table I. It can be seen that CACCu caused no speed

Entering time	Control type	# of speed overshootings	Acceleration peak (m/s²)	Acceleration RMS (m/s²)	Spacing error peak (m)	Spacing error RMS (m)	Fuel consumption (ml)
0 min	CACCu	0	0.86	0.42	1.37	0.76	47.70
	CCC	0	0.91	0.44	2.51	1.26	48.50
	ACC	1	0.94	0.47	3.33	1.71	50.00
10min	CACCu	0	0.79	0.43	1.72	0.81	31.30
	CCC	1	1.00	0.44	2.59	1.25	31.70
	ACC	1	0.99	0.45	3.33	1.58	32.70
20min	CACCu	0	0.87	0.37	1.92	0.80	30.50
	CCC	0	0.95	0.38	3.06	1.54	30.70
	ACC	0	0.95	0.38	3.80	1.60	31.30
30min	CACCu	0	1.13	0.53	3.16	1.54	39.20
	CCC	1	1.54	0.62	4.15	2.03	43.70
	ACC	2	1.47	0.67	4.96	2.47	46.50
40min	CACCu	0	1.32	0.48	2.16	0.77	23.80
	CCC	0	1.27	0.46	3.61	1.34	23.50
	ACC	2	1.40	0.50	4.38	1.67	26.10
Average	From ACC	100%	13.2%	8.5%	48.7%	49.2%	7.2%
reduction	From CCC	100%	11.5%	3.9%	36.1%	37.9%	2.5%

TABLE I
SUMMARY OF SIMULATION RESULTS IN ONE-UNCONNECTED-VEHICLE SCENARIO

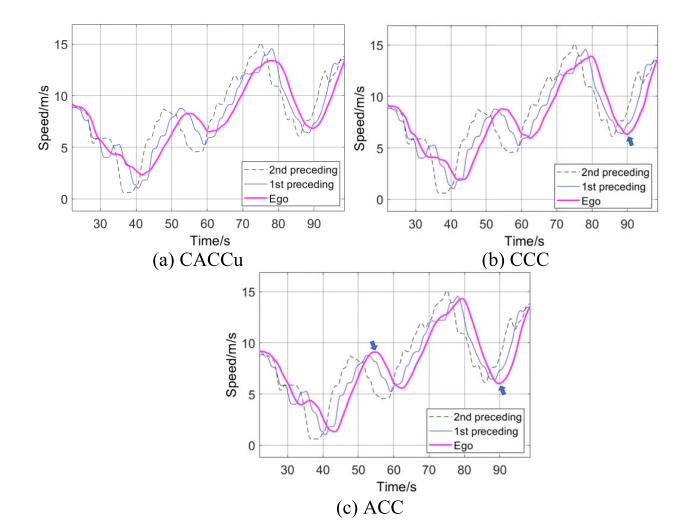


Fig. 7. The speed profiles of CACCu /CCC/ACC vehicle in the case of  $30\ \mathrm{min}.$ 

overshooting in all of the cases. This means the speed perturbation from downstream was always attenuated by the ego vehicle, thus string stability was fulfilled. By contrast, ACC encountered speed overshoots for 6 times in total, which means string stability cannot be guaranteed by ACC. CCC also failed to avoid the speed overshooting in all the cases, but it had better chance to stay string-stable than stand-alone ACC. Fig. 7 shows the vehicle speed profiles in the case 30 min under different control types. It can be found that CACCu mitigated the speed oscillation all the time while CCC overshot once at 90s and ACC overshot twice at 55s and 90s, as labeled in Fig. 7(b) and (c).

For the acceleration and spacing errors, both the peak value and RMS value are reported in Table I. In average, CACCu reduced acceleration peak value by 13.2% and RSM value by 8.5% from those of ACC, and 11.5% and 3.9% from those of CCC, showing a moderate improvement in ride comfort. On the other hand, the spacing error peak value and RSM were greatly reduced by 48.7% and 49.2% from ACC, and 36.1% and 37.9% from CCC. This indicates that CACCu has

a significantly better capability to maintain a safe inter-vehicle distance than ACC and CCC do. In addition, because of smaller acceleration and speed variation, CACCu achieved 7.2% and 2.5% fuel saving from ACC and CCC respectively.

2) Multiple Unconnected Vehicles: As aforementioned, to apply CACCu in the scenario where multiple unconnected vehicles are in between, the feedforward filter should include a combined transfer function of the multiple vehicles instead of single vehicle, that is, replacing (7) with:

$$F_0(s) = \frac{1}{G_0(s) H_0(s) s^2} T_1'(s) T_2'(s) \dots T_n'(s)$$
 (16)

where *n* is the number of unconnected vehicles. And the string stability determinant becomes:

$$SS = \|T_0(j\omega)\|_{\infty}$$

$$= \left\| \frac{H_0(j\omega)G_0(j\omega)K_0(j\omega) + D_0(j\omega)\frac{T_1'(j\omega)...T_n'(j\omega)}{T_1(j\omega)...T_n(j\omega)}}{H_0(j\omega)(1 + H_0(j\omega)G_0(j\omega)K_0(j\omega))} \right\|_{\infty}$$
(17)

Accordingly, the calculation of SSR (12) should also be substituted by:

$$SSR = \int \int \int \int p(\alpha_1, \beta_1, \varphi_1, t_{1,h}) \dots p(\alpha_n, \beta_n, \varphi_n, t_{n,h})$$

$$\xi(SS) d\alpha_1 d\beta_1 d\varphi_1 dt_{1,h} \dots d\alpha_n d\beta_n d\varphi_n dt_{n,h}$$
(18)

It is noted that the complexities of the SSR increase exponentially with the addition of the unconnected vehicles. This could bring computational issue in optimizing the parameters of  $T_1'(s)T_2'(s)\ldots T_n'(s)$  for the highest SSR. If a full design of CACCu is unavailable, a simplification is to assume homogeneous traffic, i.e., all the unconnected vehicles have the same human parameters, which leads to:

$$F_0(S) = \frac{1}{G_0(s) H_0(s) s^2} T_1'(s)^n$$
 (19)

With this simplification, an approximate SSR can be simply computed by (12).

reduction

From CCC

Entering time	Control type	# of speed overshootings	Acceleration peak (m/s²)	Acceleration RMS (m/s <sup>2</sup> )	Spacing error peak (m)	Spacing error RMS (m)	Fuel consumption (ml)
0 min	CACCu	0	0.72	0.32	1.89	0.96	36.10
	CCC	0	0.82	0.37	3.06	1.31	36.80
	ACC	0	0.87	0.38	3.04	1.39	37.00
10min	CACCu	0	0.57	0.34	1.74	0.76	30.30
	CCC	1	0.82	0.36	2.06	1.02	31.20
	ACC	1	0.76	0.35	2.50	1.36	31.20
20min	CACCu	0	1.04	0.39	3.38	1.10	32.30
	CCC	0	1.10	0.39	4.06	1.36	32.40
	ACC	0	1.12	0.39	4.47	1.64	32.30
30min	CACCu	1	1.03	0.42	3.28	1.57	29.70
	CCC	2	1.20	0.50	3.77	1.80	33.50
	ACC	5	1.19	0.54	4.24	2.14	35.80
40min	CACCu	0	0.93	0.35	1.14	0.56	17.40
	CCC	0	0.98	0.33	2.37	0.93	17.00
	ACC	0	0.88	0.35	2.92	1.26	18.00
Average	From ACC	83.3%	11.4%	8.2%	35.2%	38.0%	4.7%

TABLE II
SUMMARY OF SIMULATION RESULTS IN TWO-UNCONNECTED-VEHICLE SCENARIO

TABLE III

SUMMARY OF SIMULATION RESULTS IN THREE-UNCONNECTED-VEHICLE SCENARIO

5.8%

27.1%

24.8%

2.3%

Entering time	Control type	# of speed overshootings	Acceleration peak (m/s²)	Acceleration RMS (m/s²)	Spacing error peak (m)	Spacing error RMS (m)	Fuel consumption (ml)
0 min	CACCu	0.00	0.66	0.34	1.71	0.87	37.90
	CCC	0.00	0.72	0.36	2.92	1.37	38.60
	ACC	0.00	0.85	0.37	3.33	1.62	38.00
10min	CACCu	0.00	1.03	0.36	1.89	0.89	26.90
	CCC	1.00	1.03	0.38	3.30	1.32	28.10
	ACC	1.00	1.05	0.37	4.00	1.60	27.90
20min	CACCu	0.00	1.01	0.43	3.37	1.52	39.00
	CCC	1.00	1.11	0.42	4.06	1.67	38.10
	ACC	1.00	1.10	0.42	4.00	1.91	38.60
30min	CACCu	0.00	0.98	0.40	3.52	1.76	26.60
	CCC	2.00	1.04	0.49	3.83	2.00	29.70
	ACC	2.00	1.05	0.51	4.39	2.17	30.80
40min	CACCu	2.00	1.08	0.34	1.81	0.79	17.70
	CCC	1.00	0.99	0.33	3.09	1.31	16.60
	ACC	1.00	0.97	0.34	3.17	1.42	17.70
Average	From ACC	60.0%	5.6%	6.0%	36.0%	34.9%	3.3%
reduction	From CCC	60.0%	2.8%	4.8%	30.1%	25.9%	1.5%

In the case of two unconnected vehicles, both the full design with (16)-(18) and a simplified design of CACCu were evaluated. In full design, the optimal virtual preceding vehicles were determined to be  $T_1'(s) = T_2'(s) = (1.22, 0.26, 0, 0.99)$ . It corresponded to a critical gap of 1.3s and the maximum SSR of 97.8%. As comparison, the simplified design using (19) and (12) led to  $T_1'(s) = (1.14, 0.4, 0, 0.95)$ , corresponding to a maximum approximate SSR of 93.8% (computed by (12)). Meanwhile, the actual SSR was found to be 97.5% (computed by (18)). It is noted that although the simplified design has underestimated SSR, the obtained solution and its optimality (i.e., actual SSR) resembled the ones in full design.

66.7%

13.5%

As can be expected, these two designs of CACCu achieved very similar performances in the evaluation. For simplicity, the evaluation results with full design are reported in Table II. The desired gap of 1.3s (critical gap) was used in all the runs. Overall, CACCu led to 83% speed overshooting avoidance, 8.2% acceleration reduction, 38% spacing error

reduction and 4.7% fuel saving from ACC. It also achieved 67% speed overshooting avoidance, 5.8% acceleration reduction, 24.8% spacing error reduction and 2.3% fuel saving from CCC.

In the case of three unconnected vehicles, the full design of CACCu is infeasible because the required computation time was too long. Thus, only the simplified design was conducted. Given desired gap of 1.5s, the approximate SSR was maximized to 89.3%. Intuitively, the critical gap of CACCu in this scenario should be longer than 1.5s. However, a desired gap>1.5s means the loss of the throughput benefit over human driving which has an average desired gap of 1.5s [38]. Thus, 1.5s was assumed the maximum desired gap of ego vehicle and used in this scenario. The evaluation results for three-unconnected-vehicle scenario are summarized in Table III. CACCu led to overall 60% speed overshooting avoidance, 6% acceleration reduction, 34.9% spacing error reduction and 3.3% fuel saving from ACC, and 60% speed overshootings

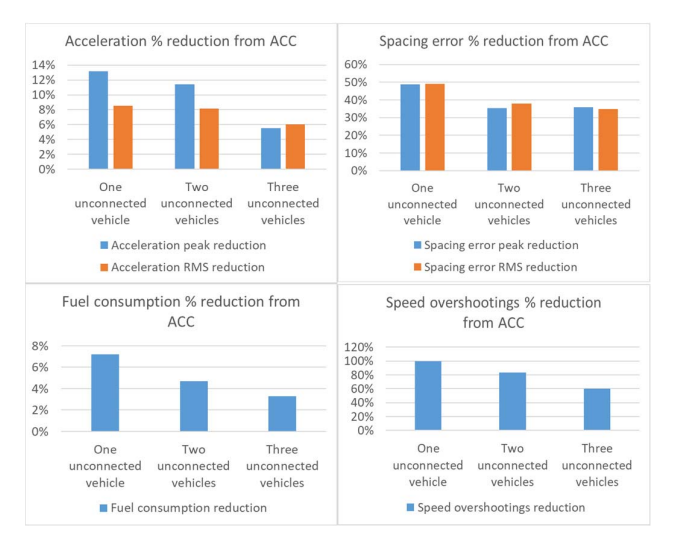


Fig. 8. Comparing the benefits of CACCu over ACC in all the three scenarios.

avoidance, 4.8% acceleration reduction, 25.9% spacing error reduction and 1.5% fuel saving from CCC.

The benefits of CACCu over ACC in all the three scenarios are compared in Fig. 8. It shows a trend that more unconnected vehicles in between would make CACCu's benefits decline. This is expected because with more unmodelled noise in human behaviors being introduced, the information of the further preceding vehicle has weaker capability to predict the motion of 1<sup>st</sup> preceding vehicle. Nevertheless, CACCu still performed consistently better than ACC and CCC in every aspect.

Generally speaking, the CACCu design described in Section II and III can be well extended to multi-unconnected-vehicle scenarios, although sometimes with approximation in determining the optimal parameters of "virtual preceding vehicles".

# V. CONCLUSION AND FUTURE RESEARCH

This paper proposed a new CACC algorithm, dubbed as CACCu, that considered unconnected vehicle in the control loop. When encountering an unconnected preceding vehicle, CACCu can utilize the communication with the further (connected) preceding vehicle to improve the response of ego vehicle. This paper started with the three-vehicle sandwich scenario (i.e., an unconnected vehicle is in between of two connected vehicles) which has the highest probability to occur among the mixed platooning scenarios. It is analytically proven that by attaching a filter of "virtual preceding vehicle" to the original CACC feedforward filter, the CACCu vehicle can stay string-stable at a gap significantly shorter than that required by ACC. Such capability is robust against the variation in unconnected vehicle's car-following behaviors, thus no beforehand identification process or extra information on the unconnected vehicles' behaviors is required.

The performance of CACCu was evaluated and compared with ACC and acceleration-based CCC, using real vehicle trajectory data from NGSIM and physics-based vehicle model from PreScan. The control design of CACCu was extended to multi-unconnected-vehicle scenarios, to evaluate CACCu in the scenarios of one, two, or three unconnected

vehicles in between. The evaluation results in all scenarios show that CACCu avoided most of speed overshootings happening to ACC and CCC. This means the string stability was greatly improved. CACCu also achieved smaller spacing error, acceleration, and fuel consumption than ACC and CCC did, indicating benefits in safety, ride comfort and energy efficiency.

A limitation of the proposed CACCu is that the complexity of controller parameterization increases exponentially when more unconnected preceding vehicle are introduced. An approximation method may need to be applied to CACCu design for better computational feasibility. While this approximation method can lead to inaccurate estimate on theoretical performance (i.e., SSR), it was still able to offered good effectiveness of the outcome.

The future work of CACCu will look into the data-driven modelling/control approaches (e.g., neuro-fuzzy predictor [50] and reinforcement learning [51]) which could adaptively handle the uncertainty and possible anomaly in preceding vehicle's behaviors. Other future researches will include evaluating the network-level benefit of CACCu, troubleshooting in edge cases using driving simulator, and exploring the benefits of communications with multiple further preceding vehicles.

#### REFERENCES

- [1] K. Bengler, K. Dietmayer, B. Farber, M. Maurer, C. Stiller, and H. Winner, "Three decades of driver assistance systems: Review and future perspectives," *IEEE Intell. Transp. Syst. Mag.*, vol. 6, no. 4, pp. 6–22, Winter 2014.
- [2] V. Milanés, S. E. Shladover, J. Spring, C. Nowakowski, H. Kawazoe, and M. Nakamura, "Cooperative adaptive cruise control in real traffic situations," *IEEE Trans. Intell. Transp. Syst.*, vol. 15, no. 1, pp. 296–305, Feb. 2014.
- [3] Z. Wang, Y. Bian, S. E. Shladover, G. Wu, S. E. Li, and M. J. Barth, "A survey on cooperative longitudinal motion control of multiple connected and automated vehicles," *IEEE Intell. Transp. Syst. Mag.*, vol. 12, no. 1, pp. 4–24, Spring 2020.
- [4] G. J. L. Naus, R. P. A. Vugts, J. Ploeg, M. J. G. van de Molengraft, and M. Steinbuch, "String-stable CACC design and experimental validation: A frequency-domain approach," *IEEE Trans. Veh. Technol.*, vol. 59, no. 9, pp. 4268–4279, Nov. 2010.
- [5] Y. Bian, Y. Zheng, W. Ren, S. E. Li, J. Wang, and K. Li, "Reducing time headway for platooning of connected vehicles via V2V communication," *Transp. Res. C, Emerg. Technol.*, vol. 102, pp. 87–105, May 2019.
- [6] A. Geiger et al., "Team AnnieWAY's entry to the 2011 grand cooperative driving challenge," *IEEE Trans. Intell. Transp. Syst.*, vol. 13, no. 3, pp. 1008–1017, Sep. 2012.
- [7] M. Wang, W. Daamen, S. P. Hoogendoorn, and B. van Arem, "Rolling horizon control framework for driver assistance systems. Part II: Cooperative sensing and cooperative control," *Transp. Res. C, Emerg. Technol.*, vol. 40, pp. 290–311, Mar. 2014.
- [8] E. van Nunen, J. Reinders, E. Semsar-Kazerooni, and N. van de Wouw, "String stable model predictive cooperative adaptive cruise control for heterogeneous platoons," *IEEE Trans. Intell. Vehicles*, vol. 4, no. 2, pp. 186–196, Jun. 2019.
- [9] E. van Nunen, M. R. J. A. E. Kwakkernaat, J. Ploeg, and B. D. Netten, "Cooperative competition for future mobility," *IEEE Trans. Intell. Transp. Syst.*, vol. 13, no. 3, pp. 1018–1025, Sep. 2012.
- [10] C. Englund et al., "The grand cooperative driving challenge 2016: Boosting the introduction of cooperative automated vehicles," *IEEE Wireless Commun.*, vol. 23, no. 4, pp. 146–152, Aug. 2016.
- Wireless Commun., vol. 23, no. 4, pp. 146–152, Aug. 2016.
  [11] H. Xing, J. Ploeg, and H. Nijmeijer, "Compensation of communication delays in a cooperative ACC system," *IEEE Trans. Veh. Technol.*, vol. 69, no. 2, pp. 1177–1189, Feb. 2020.
- [12] C. Wang, S. Gong, A. Zhou, T. Li, and S. Peeta, "Cooperative adaptive cruise control for connected autonomous vehicles by factoring communication-related constraints," *Transp. Res. Procedia*, vol. 38, pp. 242–262, Apr. 2019.

- [13] D. Wu, Y. Zhang, J. Luo, and R. Li, "Efficient data dissemination by crowdsensing in vehicular networks," in *Proc. IEEE 22nd Int. Symp. Qual. Service (IWQoS)*, May 2014, pp. 314–319.
- [14] D. Wu, J. Luo, R. Li, and A. Regan, "Geographic load balancing routing in hybrid vehicular ad hoc networks," in *Proc. 14th Int. IEEE Conf. Intell. Transp. Syst. (ITSC)*, Oct. 2011, pp. 2057–2062.
- [15] L. Cui, J. Hu, B. B. Park, and P. Bujanovic, "Development of a simulation platform for safety impact analysis considering vehicle dynamics, sensor errors, and communication latencies: Assessing cooperative adaptive cruise control under cyber attack," *Transp. Res. C, Emerg. Technol.*, vol. 97, pp. 1–22, Dec. 2018.
- [16] Z. A. Biron, S. Dey, and P. Pisu, "Real-time detection and estimation of denial of service attack in connected vehicle systems," *IEEE Trans. Intell. Transp. Syst.*, vol. 19, no. 12, pp. 3893–3902, Dec. 2018.
- [17] Z. Chen and B. B. Park, "Preceding vehicle identification for cooperative adaptive cruise control platoon forming," *IEEE Trans. Intell. Transp. Syst.*, vol. 21, no. 1, pp. 308–320, Jan. 2019.
- [18] Q. Wang, X. Yang, Z. Huang, and Y. Yuan, "Multi-vehicle trajectory design during cooperative adaptive cruise control platoon formation," *Transp. Res. Rec., J. Transp. Res. Board*, vol. 2674, no. 4, pp. 30–41, Apr. 2020.
- [19] A. Duret, M. Wang, and A. Ladino, "A hierarchical approach for splitting truck platoons near network discontinuities," *Transp. Res. Procedia*, vol. 38, pp. 627–646, Feb. 2019.
- [20] J. Hu, H. Wang, X. Li, and X. Li, "Modelling merging behaviour joining a cooperative adaptive cruise control platoon," *IET Intell. Transp. Syst.*, vol. 14, no. 7, pp. 693–701, Jul. 2020.
- [21] H. Liu, X. Kan, S. E. Shladover, X.-Y. Lu, and R. E. Ferlis, "Modeling impacts of cooperative adaptive cruise control on mixed traffic flow in multi-lane freeway facilities," *Transp. Res. C, Emerg. Technol.*, vol. 95, pp. 261–279, Oct. 2018.
- [22] J. Lioris, R. Pedarsani, F. Y. Tascikaraoglu, and P. Varaiya, "Platoons of connected vehicles can double throughput in urban roads," *Transp. Res. C, Emerg. Technol.*, vol. 77, pp. 292–305, Apr. 2017.
- [23] S. Shladover et al., "Cooperative adaptive cruise control (CACC) for partially automated truck platooning: Final report," Federal Highway Admin., Explor. Adv. Res. Program, Washington, DC, USA, Tech. Rep., 2018. [Online]. Available: https://escholarship.org/uc/item/260060w4
- [24] A. Talebpour and H. S. Mahmassani, "Influence of connected and autonomous vehicles on traffic flow stability and throughput," *Transp. Res. C, Emerg. Technol.*, vol. 71, pp. 143–163, Oct. 2016.
- [25] S. E. Shladover, D. Su, and X.-Y. Lu, "Impacts of cooperative adaptive cruise control on freeway traffic flow," *Transp. Res. Rec., J. Transp. Res. Board*, vol. 2324, no. 1, pp. 63–70, Jan. 2012.
- [26] D. Jia, D. Ngoduy, and H. L. Vu, "A multiclass microscopic model for heterogeneous platoon with vehicle-to-vehicle communication," *Trans*portmetrica B, Transp. Dyn., vol. 7, no. 1, pp. 311–335, Dec. 2019.
- [27] J. Ma, F. Zhou, and M. J. Demetsky, "Evaluating mobility and sustainability benefits of cooperative adaptive cruise control using agent-based modeling approach," in *Proc. IEEE Syst. Inf. Eng. Design Symp.*, Apr. 2012, pp. 74–78.
- [28] E. Talavera, A. Díaz-Álvarez, F. Jiménez, and J. Naranjo, "Impact on congestion and fuel consumption of a cooperative adaptive cruise control system with lane-level position estimation," *Energies*, vol. 11, no. 1, p. 194, Jan. 2018.
- [29] J. Ploeg, E. Semsar-Kazerooni, G. Lijster, N. van de Wouw, and H. Nijmeijer, "Graceful degradation of cooperative adaptive cruise control," *IEEE Trans. Intell. Transp. Syst.*, vol. 16, no. 1, pp. 488–497, Feb. 2015.
- [30] J. I. Ge and G. Orosz, "Dynamics of connected vehicle systems with delayed acceleration feedback," *Transp. Res. C, Emerg. Technol.*, vol. 46, pp. 46–64, Sep. 2014.
- [31] L. Zhang and G. Orosz, "Beyond-line-of-sight identification by using vehicle-to-vehicle communication," *IEEE Trans. Intell. Transp. Syst.*, vol. 19, no. 6, pp. 1962–1972, Jun. 2018.
- [32] N. Chen, M. Wang, T. Alkim, and B. van Arem, "A robust longitudinal control strategy of platoons under model uncertainties and time delays," *J. Adv. Transp.*, vol. 2018, pp. 1–13, Jan. 2018.
- [33] J. I. Ge and G. Orosz, "Connected cruise control among humandriven vehicles: Experiment-based parameter estimation and optimal control design," *Transp. Res. C, Emerg. Technol.*, vol. 95, pp. 445–459, Oct. 2018.
- [34] J. I. Ge, S. S. Avedisov, C. R. He, W. B. Qin, M. Sadeghpour, and G. Orosz, "Experimental validation of connected automated vehicle design among human-driven vehicles," *Transp. Res. C, Emerg. Technol.*, vol. 91, pp. 335–352, Jun. 2018.

- [35] A. M. H. Al-Jhayyish and K. W. Schmidt, "Feedforward strategies for cooperative adaptive cruise control in heterogeneous vehicle strings," *IEEE Trans. Intell. Transp. Syst.*, vol. 19, no. 1, pp. 113–122, Jan. 2018.
- [36] S. E. Shladover, C. Nowakowski, X.-Y. Lu, and R. Ferlis, "Cooperative adaptive cruise control: Definitions and operating concepts," *Transp. Res. Rec., J. Transp. Res. Board*, vol. 2489, no. 1, pp. 145–152, Jan. 2015.
- [37] J. I. Ge and G. Orosz, "Optimal control of connected vehicle systems with communication delay and driver reaction time," *IEEE Trans. Intell. Transp. Syst.*, vol. 18, no. 8, pp. 2056–2070, Aug. 2017.
- [38] T. J. Ayres, L. Li, D. Schleuning, and D. Young, "Preferred time-headway of highway drivers," in *Proc. IEEE Intell. Transp. Syst. (ITSC)*, Aug. 2001, pp. 826–829.
- [39] G. Orosz, R. E. Wilson, and G. Stépán, "Traffic jams: Dynamics and control," *Philos. Trans. Roy. Soc. A*, vol. 368, no. 1928, pp. 4455–4479, 2010
- [40] A. Mehmood and S. M. Easa, "Modeling reaction time in car-following behaviour based on human factors," *Int. J. Appl. Sci. Eng. Technol.*, vol. 3, no. 9, pp. 325–333, 2009.
- [41] I. G. Jin, G. Orosz, D. Hajdu, T. Insperger, and J. Moehlis, "To delay or not to delay—Stability of connected cruise control," in *Time Delay Systems*. New York, NY, USA: Springer, 2017, pp. 263–282.
- [42] R. Rajamani, Vehicle Dynamics and Control. New York, NY, USA: Springer, 2006.
- [43] M. R. I. Nieuwenhuijze, T. van Keulen, S. Oncu, B. Bonsen, and H. Nijmeijer, "Cooperative driving with a heavy-duty truck in mixed traffic: Experimental results," *IEEE Trans. Intell. Transp. Syst.*, vol. 13, no. 3, pp. 1026–1032, Sep. 2012.
- [44] L. Xiao and F. Gao, "Practical string stability of platoon of adaptive cruise control vehicles," *IEEE Trans. Intell. Transp. Syst.*, vol. 12, no. 4, pp. 1184–1194, Dec. 2011.
- [45] V. Alexiadis, J. Colyar, J. Halkias, R. Hranac, and G. McHale, "The next generation simulation program," *Inst. Transp. Eng. J.*, vol. 74, no. 8, pp. 22–26, 2004.
- [46] M. Tideman, "Scenario-based simulation environment for assistance systems," ATZautotechnology, vol. 10, no. 1, pp. 28–32, Jan. 2010.
- [47] H. A. Rakha, K. Ahn, K. Moran, B. Saerens, and E. V. D. Bulck, "Virginia tech comprehensive power-based fuel consumption model: Model development and testing," *Transp. Res. D, Transp. Environ.*, vol. 16, no. 7, pp. 492–503, Oct. 2011.
- [48] V. Punzo, M. T. Borzacchiello, and B. Ciuffo, "On the assessment of vehicle trajectory data accuracy and application to the next generation SIMulation (NGSIM) program data," *Transp. Res. C, Emerg. Technol.*, vol. 19, no. 6, pp. 1243–1262, Dec. 2011.
- [49] J. Hasch, E. Topak, R. Schnabel, T. Zwick, R. Weigel, and C. Waldschmidt, "Millimeter-wave technology for automotive radar sensors in the 77 GHz frequency band," *IEEE Trans. Microw. Theory Techn.*, vol. 60, no. 3, pp. 845–860, Mar. 2012.
- [50] Y.-C. Lin and H. L. T. Nguyen, "Adaptive neuro-fuzzy predictor-based control for cooperative adaptive cruise control system," *IEEE Trans. Intell. Transp. Syst.*, vol. 21, no. 3, pp. 1054–1063, Mar. 2020.
- [51] W. Gao, J. Gao, K. Ozbay, and Z.-P. Jiang, "Reinforcement-learning-based cooperative adaptive cruise control of buses in the Lincoln tunnel corridor with time-varying topology," *IEEE Trans. Intell. Transp. Syst.*, vol. 20, no. 10, pp. 3796–3805, Oct. 2019.



Zheng Chen (Graduate Student Member, IEEE) received the B.S. and M.S. degrees in mechanical engineering from Hunan University, China, in 2014 and 2017, respectively, and the Ph.D. degree in civil engineering from the University of Virginia, Charlottesville, VA, USA, in 2020. His research interests include dynamics and control of connected vehicle systems.



Byungkyu Brian Park (Senior Member, IEEE) is currently a Professor with the Link Lab and the Department of Engineering Systems and Environment, University of Virginia. He has published more than 160 journal articles and conference papers in the areas of transportation system operations and managements, and intelligent transportation systems. His research interests include cyber-physical system for transportation, stochastic optimization, and connected and automated vehicle.